PROTEINS: Structure, Function, and Genetics 3:1–17 (1988)

Two Trifluoperazine-Binding Sites on Calmodulin Predicted From Comparative Molecular Modeling With Troponin-C

Natalie C.J. Strynadka and Michael N.G. James
Medical Research Council of Canada Group in Protein Structure and Function, Department of Biochemistry, University of Alberta, Edmonton, Alberta, Canada T6G 2H7

ABSTRACT **Among the known regulatory proteins that are conformationally sensitive to the binding of calcium ions, calmodulin and troponin-C have the greatest primary sequence homology. This observation has led to the conclusion that the most accurate predicted molecular model of calmodulin would be based on the X-ray crystallographic coordinates of the highly refined structure of turkey skeletal troponin-C. This paper describes the structure of calmodulin built from such a premise. The resulting molecular model was subjected to conjugate gradient energy minimization to remove unacceptable intramolecular non-bonded contacts. In the analysis of the resulting structure, many features of calmodulin, including the detailed conformation of the Ca^{2+}-binding loops, the amino- and carboxy-terminal hydrophobic patches of the Ca^{2+}-bound form, and the several clusters of acidic residues can be reconciled with much of the previously published solution data. Calmodulin is missing the N-terminal helix characteristic of troponin-C. The deletion of three residues from the central helical linker (denoted D/E in troponin-C) shortens the molecule and changes the orientation of the two domains of calmodulin by 60° relative to those in troponin-C. The molecular model has been used to derive two possible binding sites for the antipsychotic drug trifluoperazine, a potent competitive inhibitor of calmodulin activity.**

Key words: computer modeling, trifluoperazine, conformational change, calcium binding proteins, hydrophobic binding interactions

INTRODUCTION

Calmodulin (CaM) is an ubiquitous, small, acidic protein of molecular weight 16,700.[1] It has four calcium-binding sites, two in the amino-terminal (N-terminal) domain with $K_d \sim 10^{-5}$ M and two in the carboxy-terminal (C-terminal) domain of slightly higher Ca^{2+} binding affinity.[2–4] CaM plays a pivotal role in many Ca^{2+}-dependent intracellular functions, including the regulation of the reactions of a number of enzymes: phosphodiesterase,[5,6] myosin light chain kinase,[8–10] erythrocyte Ca^{2+}-ATPase,[11,12] brain adenylate cyclase,[13–15] phosphorylase kinase,[16] and nicotinamide dinucleotide kinase.[7]

The Ca^{2+}-saturated form of CaM is the active form. The enhancement of enzymatic activity in all these systems is thought to be due to conformational changes in the enzymes induced upon binding the four-calcium ($4Ca^{2+}$) form of CaM. Therefore, Ca^{2+} efflux/influx of the cell controls CaM activation which in turn modulates these intracellular processes. Additionally, CaM-mediated activation of these enzymes can be inhibited by various drugs, including those of the phenothiazine family.[17,18]

Structurally, CaM belongs to the family of calcium-binding proteins including troponin-C (TnC), parvalbumin and the intestinal Ca^{2+}-binding protein. These proteins exhibit a common structural motif of helix-loop-helix frequently referred to as the EF-hand.[19] The EF-hand comprises approximately 33 residues in a linear sequence. The central Ca^{2+}-binding loop has 12 residues, and the two flanking α-helices have from 10 to 14 residues. The angle between the helical axes, E-F, varies from approximately 110° in the calcium-filled conformation to between 133° to 150° in the calcium-free conformation.[20] In the Ca^{2+}-filled conformation, there is a very strong conservation of tertiary structure of the binding loops among the several proteins whose crystal structures have been refined.[21]

The structure of TnC from turkey skeletal muscle has been refined to 2.0 Å resolution.[22] The present crystallographic agreement factor, $R(= \Sigma||F_o| - |F_c||/\Sigma|F_o|$, where $|F_o|$ and $|F_c|$ are the observed and calculated structure factor amplitudes) is 0.155. The root mean square deviations of the refined structure from standard amino-acid geometry are small. The current TnC structure consists of 160 amino acids (there is no interpretable electron density for the first residue and the last side chain of TnC), two Ca^{2+} ions in the high-affinity sites of the Ca^{2+}/Mg^{2+} C-terminal domain and 156 ordered solvent molecules refined as oxygen atoms. The N-terminal domain has no Ca^{2+} ions bound, and the helices have markedly different interaxial angles to the equivalent helices of the C-terminal domain.[20,23,24] It has been proposed that the crystal structure of TnC represents the conformation

Received August 10, 1987; accepted October 15, 1987.

Address reprint requests to Dr. Michael N.G. James, Department of Biochemistry, University of Alberta, Edmonton, Alberta, Canada T6G 2H7.

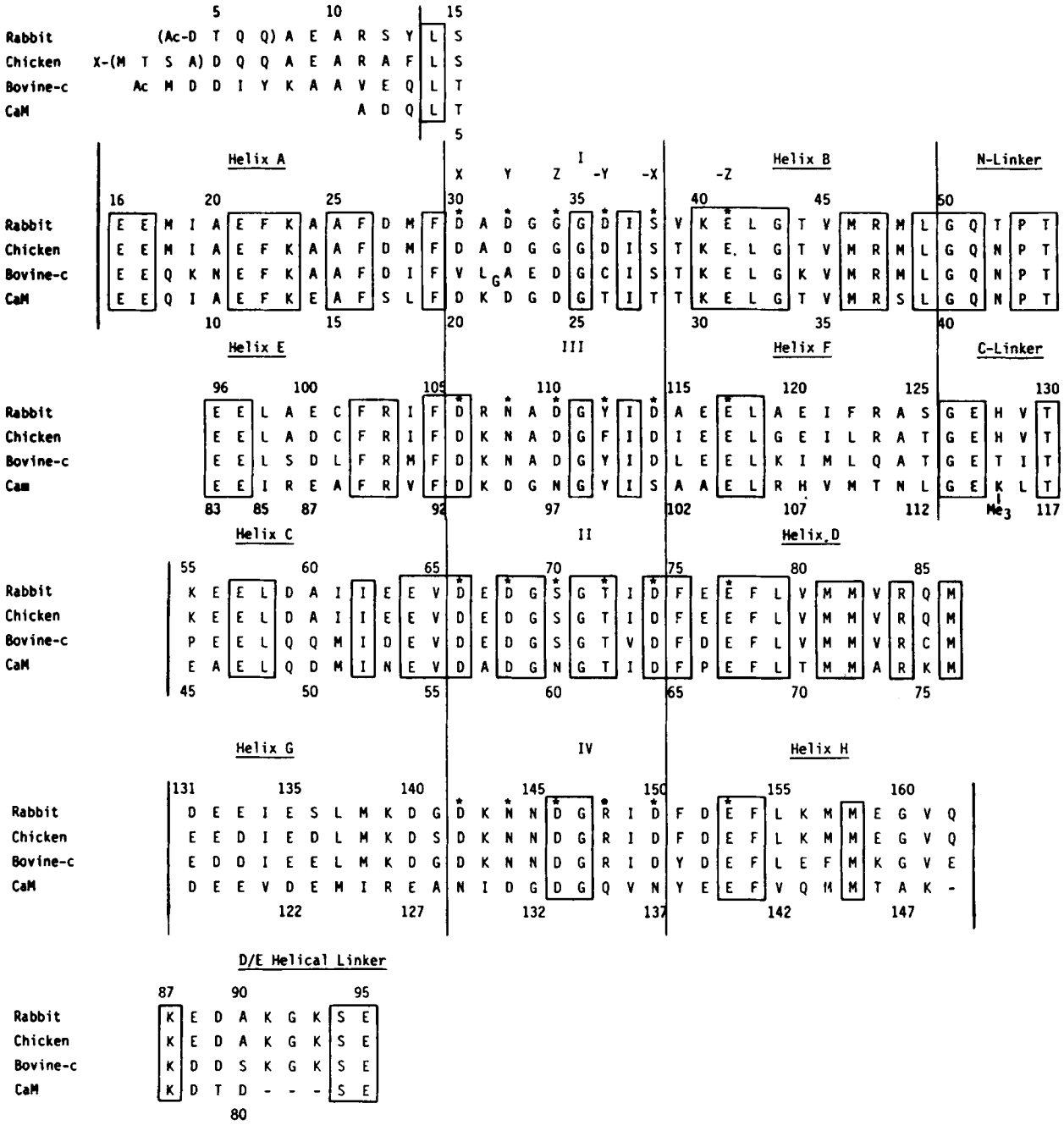

Fig. 1. The amino acid sequence alignment of calcium-modulated proteins based on the tertiary structure of TnC. The sequences are of rabbit skeletal TnC,[64] chicken skeletal TnC,[65] bovine cardiac TnC,[66] and bovine brain CaM.[67] The amino acid numbering is that of chicken skeletal TnC on top and bovine brain CaM below. The segments of the molecule are labeled according to the scheme given in Figure 2a. Residues involved in coordinating Ca^{2+} are indicated by an asterisk (*). The sequence comparison has been made so that the homologous pairs of EF hands are aligned, i.e., binding loop I with III and binding loop II with IV. The vertical lines demark the initiation and termination of helices. Note the ends of the loops and the following helices overlap by three residues. Those residues that are identical in all four proteins are enclosed in boxes.

of TnC in the relaxed state of muscle.[24] Thus, on release of Ca^{2+} from the sarcoplasmic reticulum, the N-terminal domain of TnC binds two calcium ions, triggering the contraction event.[23] It is the $4Ca^{2+}$ form of TnC that we have used as a template to construct the model of CaM.

Not only does CaM have a high degree of sequence identity with TnC (51%), they also share many similar physicochemical properties.[25,26] In fact, bovine brain CaM can substitute effectively for TnC in activating the actomyosin ATPase system of skeletal muscle.[27,28] Therefore, the refined crystal structure

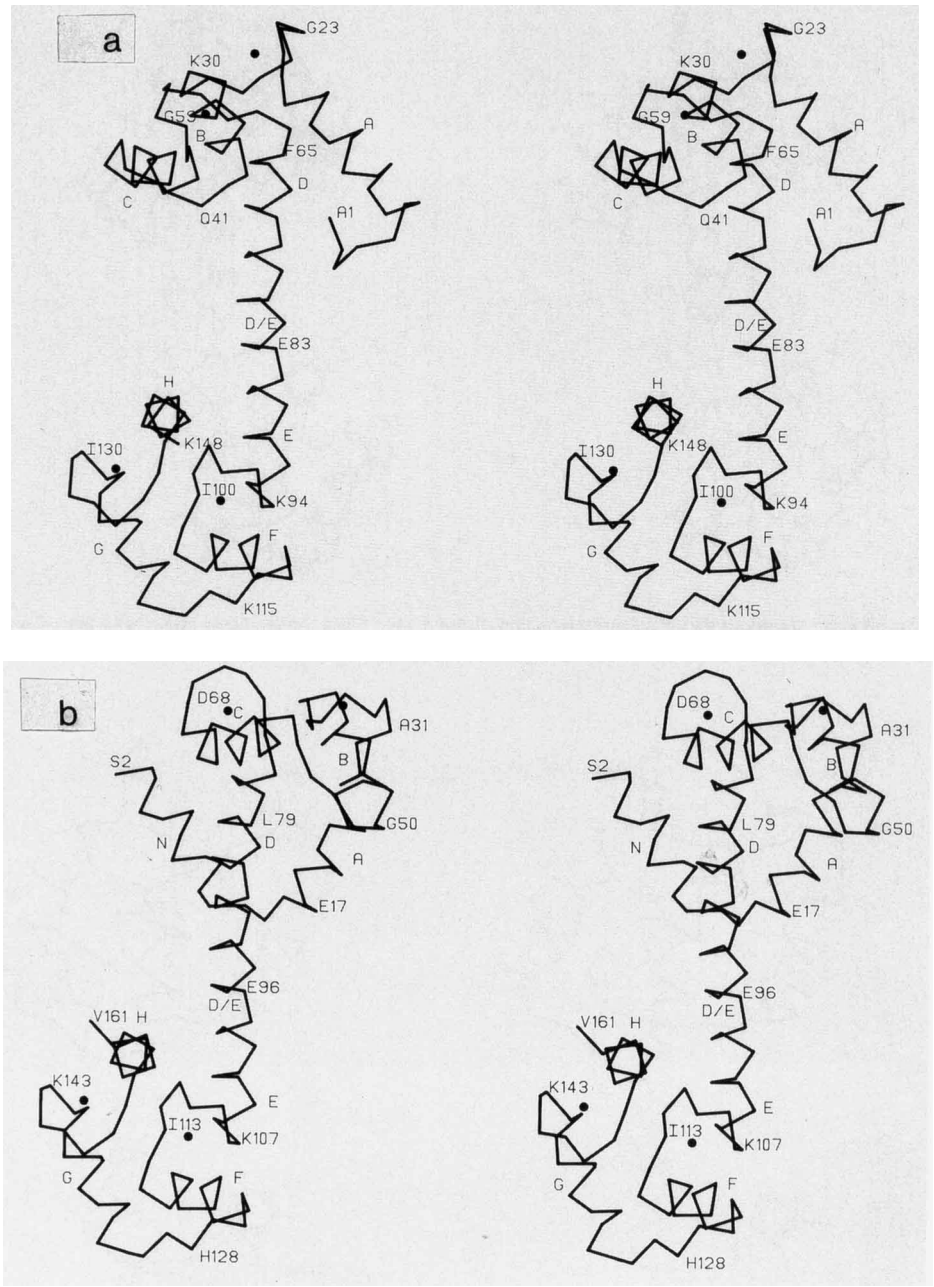

Fig. 2. **a**: A stereo representation of the c-α backbone of the calcium-saturated ($4Ca^{2+}$) model of bovine brain CaM. Helices are labeled appropriately (A,B,C,D, D/E, E,F,G,H) and coincide with Figure 1. Calciums are represented by black spheres. **b**: A stereo view of the c-α backbone of calcium-saturated ($4Ca^{2+}$) turkey skeletal troponin-C. Labeling as for Figure 2a. For comparison, the orientation of the C-terminal domain is the same as that of the $4Ca^{2+}$ CaM model.

of skeletal TnC should provide an excellent basis for the construction of a model for CaM.

A preliminary report of the crystal structure of CaM[29] has confirmed that indeed it has a molecular architecture closely resembling that of TnC.[20,24] However, at present, neither the details of the individual side chain conformations nor of the calcium binding loop structures are available in published or accessible atomic coordinates. Therefore we have built a complete atomic model of CaM in order to provide further structural data for the interpretation of the many physical measurements for that molecule in solution and to evaluate our current model-building procedures. Two previous model-building attempts on the CaM structure have been published but these were based upon the structures of carp parvalbumin and bovine intestinal Ca^{2+}-binding protein.[30,31] The description of the present model (and ultimately the

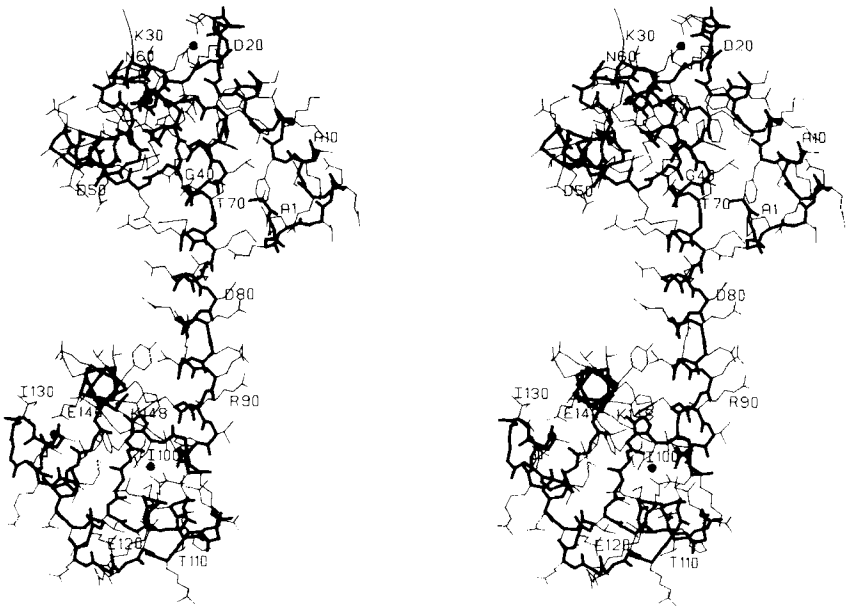

Fig. 3. An all atom stereographic stick representation of the $4Ca^{2+}$ CaM model. Main chain is in thick lines, side chains are in thin lines. Numbering is as in Figure 1.

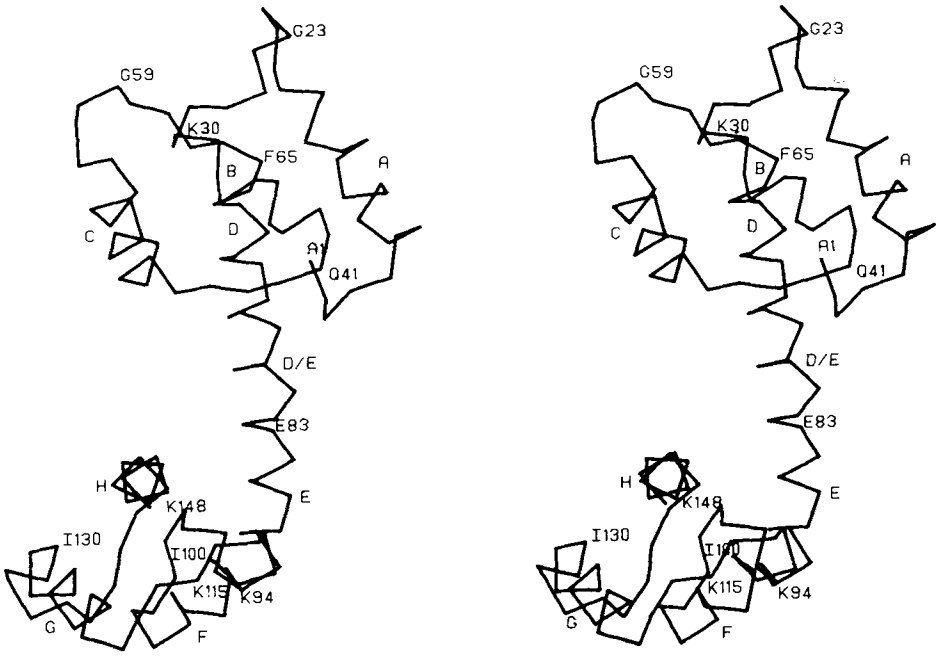

Fig. 4. A stereoview of the c-α backbone of the calcium-free ($0Ca^{2+}$) CaM model. Numbering and naming of helices is as in Figure 1.

comparison of our model with the refined structure of CaM) may reveal a more faithful prediction of the CaM structure. Our modeling has not been influenced in any way by prior knowledge of the CaM atomic coordinates. We discuss the validity of the modeling in terms of the known experimental data on CaM function.

MATERIALS AND METHODS

The amino acid sequences of bovine brain CaM and chicken skeletal TnC have been aligned as shown in Figure 1. The sequence of turkey skeletal TnC is not available but amino-acid composition analysis and the electron density from the X-ray crystallographic

Fig. 5. **a**: A stereo representation of calcium-binding sites I and II in $4Ca^{2+}$ CaM model. Calcium-coordinating side chains or main chain carbonyls are shown as thick lines. Calciums and waters are shown as large and small black spheres, respectively. Calcium-residue coordination is represented by a dashed line. **b**: A stereo representation of calcium-binding sites III and IV. Labeling is as for Figure 5a.

TABLE I. Noncovalent Interactions in CaM

	N-terminal domain	C-terminal domain
Total solvent-accessible surface area (Å^2)		
Ca^{2+}-bound	5,461	5,340
Ca^{2+}-free	4,926	4,720
Change (Å^2)	−535	−620
No. main chain hydrogen bonds		
Ca^{2+}-bound	58	48
Ca^{2+}-free	56	47
Potential ion pairs		
Ca^{2+}-bound	Arg 37-Glu 45 Arg 74-Glu 54	Arg 106-Asp 118
Ca^{2+}-free	Lys 30-Glu 31 Arg 37-Glu 45 Arg 74-Glu 54 Lys 75-Glu 47 Lys 75-Asp 78	Arg 106-Asp 118 Arg 106-Asp 122 Lys 148-Glu 120

analysis indicate only two amino acid differences. For one of these in the turkey TnC a glutamate replaces an alanine at position 99.

In order to construct a CaM model the sequence alignment of Figure 1 and the computer program MUTATE (R.J. Read, unpublished) were used to replace the side chains of the $4Ca^{2+}$-TnC model[23] with the homologous side chains of CaM. This replacement was done by retaining atoms common to the native and mutated residues and then building any additional atoms required in the standard conformation for that amino acid residue. The two most significant structural changes are the loss of the first ten residues of the N-terminal helix and a three-residue Lys-Gly-Lys deletion from the D/E interdomain helical linker of TnC (see Fig. 1). This internal deletion was compensated by calculating a rotational matrix and a translation vector to accomplish the joining of the two CaM residues directly preceding and following the deletion (Asp80, Ser81). In TnC, the C-terminal residues Gly160, Val161, and Gln162 depart from an α-helical conformation owing to an intermolecular contact in the crystal structure. In our model of CaM, the C-terminal three residues (Thr146, Ala147, Lys148) of helix H (see Fig. 1) were given an α-helical conformation.

In order to relieve unacceptably close van der Waals contacts and to correct for the inappropriate geometry obtained when mutating a glutamic acid to a proline residue at position 66, 750 cycles of conjugate-gradient energy minimization were carried out on the modeled CaM. The energy minimization was done using the GROMOS library of computer programs.[32] The potential function used in this suite of programs

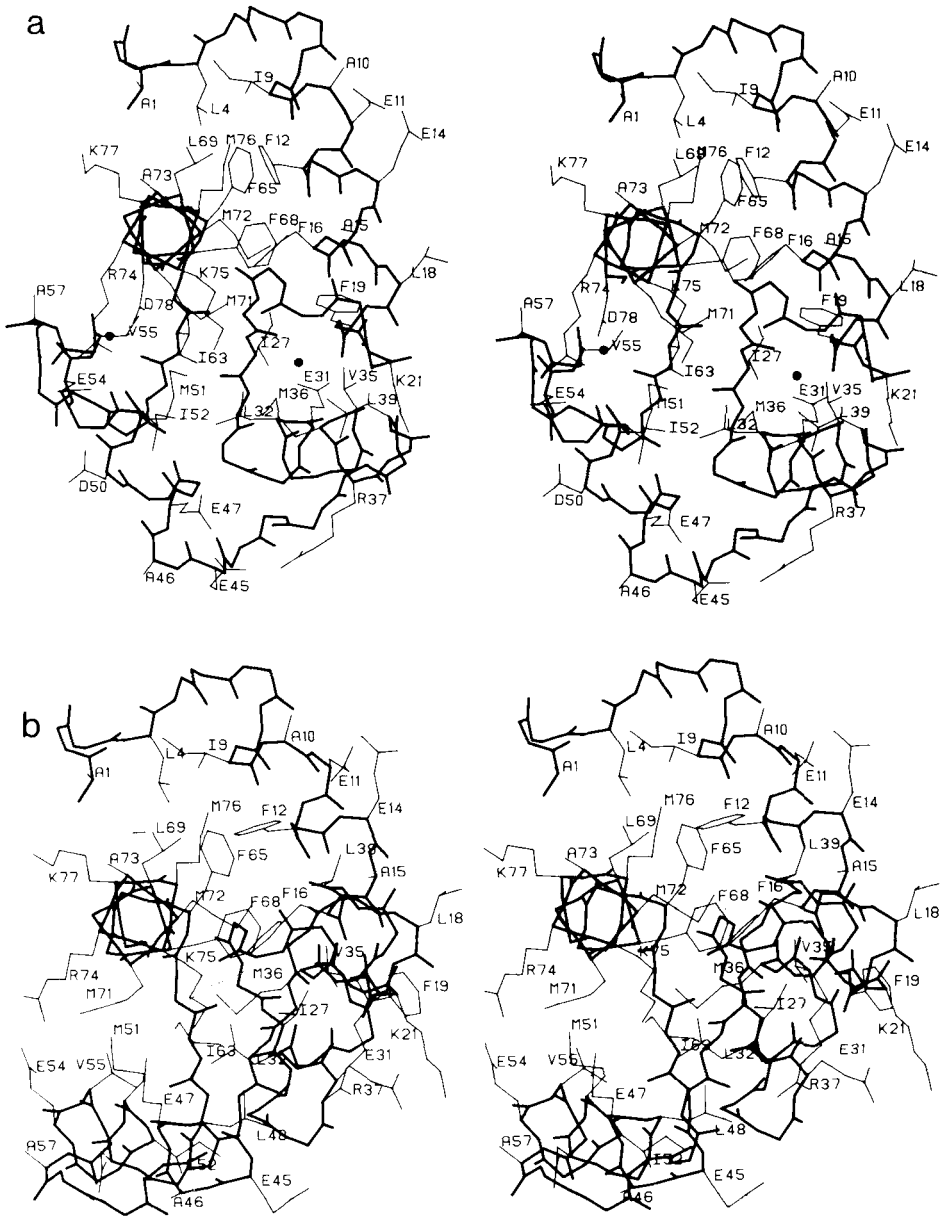

Fig. 6. **a**: A stereo view of the N-terminal domain in the "open" $4Ca^{2+}$ CaM model. The orientation is looking down the D-helix. Main chain atoms are thick lines; side chains are thin lines. Calcium ions are denoted as black spheres. For clarity, only hydrophobic residues and select charged residues are represented with side chains. **b**: A stereo view of the N-terminal domain in the "closed" $0Ca^{2+}$ CaM model. The orientation is, again looking down the D-helix. Labeling is as for Figure 6b.

is essentially that described by Karplus and Van Gunsteren.[33] The potential function parameters were those of set 37 D of GROMOS with an 8 Å cutoff. All bond lengths and angles were optimized to fit the potential used in the energy minimization. Electrostatic charges, including the contributions from calcium ions, were not considered in the calculations. Calcium-ligand binding distances within loops I–IV were idealized using a suite of programs on a Silicon Graphic (Iris) workstation.

An approach similar to that outlined above was used to construct a model of the calcium-free form of calmodulin. The calcium-free conformation of the N-terminal domain of the highly refined two-calcium turkey TnC structure was used as a template to model a calcium-free N terminus of calmodulin, again using the sequence alignment of Figure 1 and replacing side chains with the MUTATE program. In turn, the calcium-free conformation of the N-terminal domain was used as a template to model a calcium-free C-

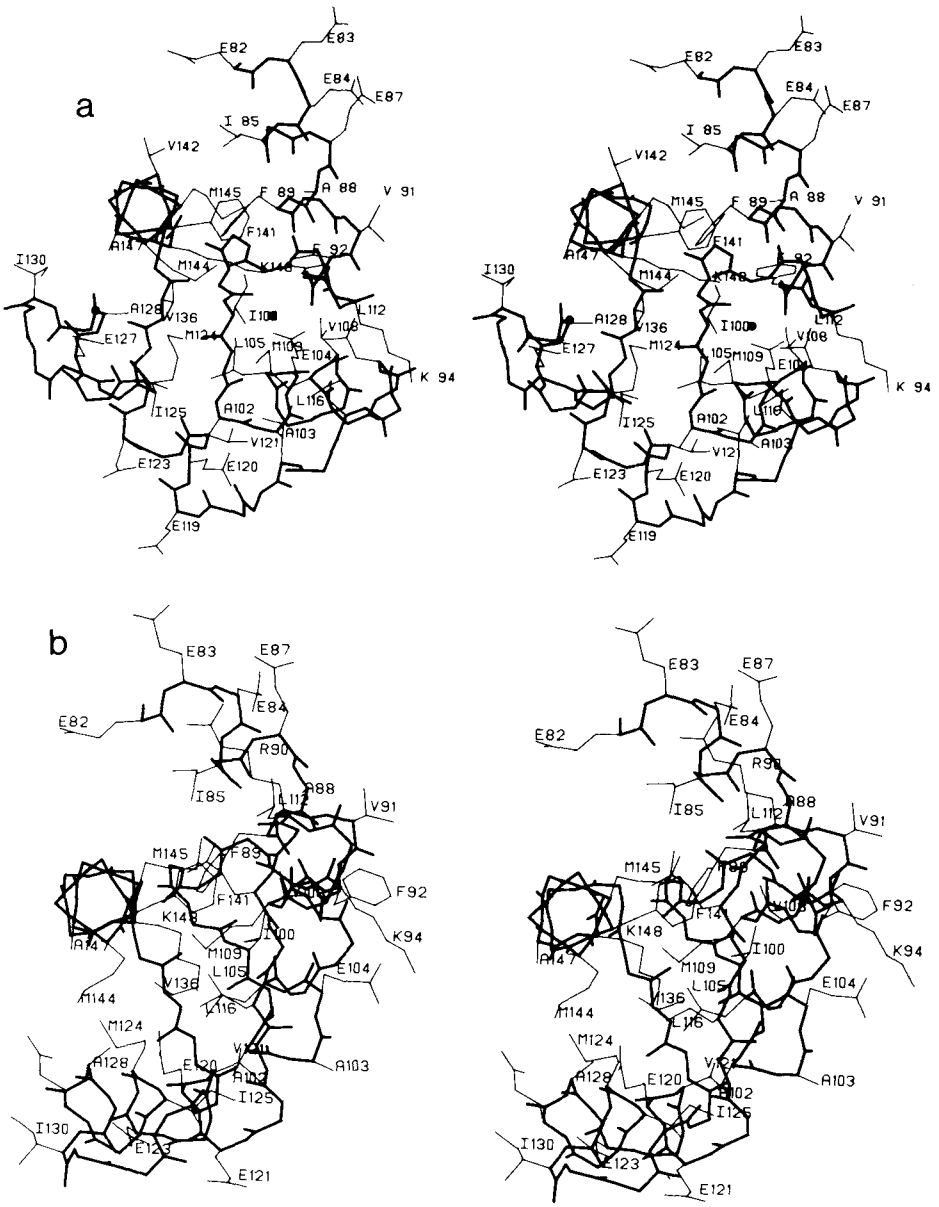

Fig. 7. **a**: A stereo representation of the C-terminal domain in the "open" $4Ca^{2+}$ CaM model. The orientation is looking down the H-helix, analogous to the view in Figure 6a. Main chain atoms are thick lines; side chains are in thin lines. Calcium ions are denoted as black spheres. For clarity, only side chains for hydrophobic and select charged residues have been represented. **b**: A stereo view of the C-terminal domain in the "closed" $0Ca^{2+}$ CaM model. Orientation and labeling is as for Figure 7a.

terminal domain, with residues of helices E, F, G, and H substituting into the analogous site in helices A, B, C, and D, respectively. The appropriate transformation was used to rejoin the domains to yield a calcium-free CaM model. Finally, 1,000 steps of conjugate gradient energy minimization were carried out on this CaM ($0Ca^{2+}$) model.

RESULTS AND DISCUSSION

It is clear from the amino-acid sequence alignment of Figure 1 that there is extensive homology among these several Ca^{2+}-sensitive regulatory proteins. The alignment of the sequences is facilitated by the obvious sequences of the EF hands.[19] It is also clear that the AB hand has high homology with the EF hand. The two major differences between TnC and CaM, the extra 10 N-terminal residues in TnC and the deletion of the Lys-Gly-Lys tripeptide in the D/E helical linker of CaM, can be easily accommodated. The extensive homology bodes well for successful comparative molecular modeling.[34,35] Unlike some regions within the serine proteinases,[35] there are no

TABLE II. Solvent Accessibility of Selected Residues of Calmodulin†

	N-terminal domain accessibility (Å^2)				C-terminal domain accessibility (Å^2)		
Residue	$+Ca^{2+}$	$-Ca^{2+}$	$\delta(-Ca^{2+}/+Ca^{2+})$	Residue	$+Ca^{2+}$	$-Ca^{2+}$	$\delta(-Ca^{2+}/+Ca^{2+})$
Phe 12$^+$	25	5	−20	Phe 89	18	0	−18
Phe 16	17	0	−17	*Phe 92$^+$	61	48	−13
*Phe 19$^+$	63	64	1	Phe 141	0	0	0
Phe 65	55	24	−31	Leu 105	12	3	−9
Phe 68	0	0	0	*Leu 112$^+$	112	53	−59
*Leu 18$^+$	131	141	10	Leu 116	42	34	−8
Leu 32	11	1	−10	*Ala 88$^+$	27	22	−5
*Leu 39$^+$	100	28	−72	Ala 128	9	0	−9
Leu 48	3	12	−9	*Val 91$^+$	110	108	−2
Leu 69	18	19	1	*Val 108$^+$	41	0	−41
*Ala 15$^+$	21	17	−4	Val 121	5	2	−3
*Val 35$^+$	36	0	−36	Val 136	2	1	−1
Val 55	16	18	2	Val 142	52	51	−1
Ile 9	16	16	0	Ile 85	107	88	−19
Ile 27	3	3	0	Ile 100	3	4	1
Ile 52	13	46	23	Ile 125	16	44	28
*Met 36$^+$	66	4	−62	*Met 109$^+$	51	2	−49
*Met 71$^+$	23	6	−20	Met 124$^+$	35	24	−9
*Met 72$^+$	39	0	−39	*Met 144$^+$	41	10	−31
Met 76$^+$	41	29	−12	*Met 145$^+$	57	12	−45
*Glu 11	120	96	−24	*Glu 84	187	197	−10
*Glu 14	118	129	11	*Glu 87	162	164	2
Lys 75	117	12	−105	Lys 148	225	64	−161

†Residues labeled with an asterisk are involved in binding trifluoperazine; residues denoted by + sign comprise the hydrophobic patch of each domain.

segments in which the TnC and CaM alignment are in doubt.

The extensive homology was evident even in the initial model obtained after replacing the TnC side chains with the aligned side chains of CaM. There were very few too short interatomic contacts even before the energy minimization. The only serious mainchain stereochemical problem was at position 66 in CaM in which a proline replaced a glutamate in TnC. Energy minimization compensated and corrected the stereochemistry at Pro66 without seriously altering the loop II conformation (root mean square difference in coordinates for the main chain atoms of the 12 residues of the loop before and after energy minimization was .10 Å). That proline 66 would be a conservative change was predicted much earlier by Kretsinger.[19] It is straightforward to accommodate a proline at the N-terminus of a helix. The overall root mean square change in coordinates as a result of energy minimization was 0.35 Å with the largest movements associated with residues Pro66 and His107. The total drop in potential energy was from 1.05×10^4 kJ/mol to -6.9×10^3 kJ/mol. This energy does not include any electrostatic contributions from charged side chains nor does it include a contribution from the Ca^{2+} ions that were positioned to superimpose closely with the equivalent observed Ca^{2+} ion positions in the C-terminal domain of TnC. The protein ligands for each of the Ca^{2+} ions were adjusted using the interactive computer graphics package MMS (S. Dempsey) for the Silicon Graphic IRIS 3030.

Caveats Concerning This Predicted Model of CaM

Before discussing the predicted structure of CaM and detailing how we feel this model provides molecular explanations for many of the solution properties of CaM, we would like to outline briefly how our model may differ from the refined structure of CaM in two regions.

Firstly, the polypeptide segment of the five residues that precede helix A could have a very different conformation. We have retained the conformation of those homologous residues in TnC primarily because there is a suitable hydrophobic site to accomodate the side chain of Leu4 of CaM in a position similar to that of Leu14 in TnC. From the preliminary publication on the crystal structure of CaM,[29] this segment of chain Ala1-Thr5 looks different from that of our model.

The second expected major difference between the structure that we have predicted and that from the refined crystal structure is in the interhelical angles of the helix-loop-helix motifs. The solution of the structure of TnC showed that this is a region of great conformational variability because differences of up to 40° exist between the Ca^{2+}-free conformation and the Ca^{2+}-bound conformation.[20,23] Thus, in our model of CaM, the interhelical angles for those helices flanking Ca^{2+}-binding sites I and III (A B and E F)

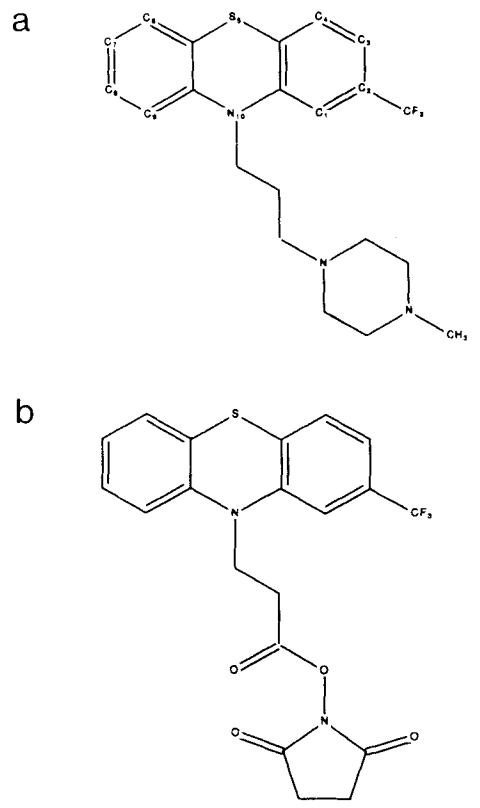

Fig. 8. **a**: The chemical configuration of trifluoperazine (TFP). Molecular coordinates used for modeling were those of McDowell.[68] **b**: The chemical configuration of 10-(3-propionyloxysuccinimide)-2-(trifluoromethyl)phenothiazine (POS-TP).[69]

are 107° and for those helices flanking Ca^{2+}-binding sites II and IV (C D and G H) the angle is 110°. These are, of course, the values for the interhelical angles in the $4Ca^{2+}$ model of TnC on which our structure is based.[23,24] These angles differ from those reported in the initial CaM structural paper which had values for the interhelical angles of 92° (A B), 96° (C D), 97° (E F), and 107° (G H). These angles could change upon refinement of the structure, but in any case it means that the N-domain and the C-domain in the crystal structure are in even more open conformations than our model would suggest. These differences in interhelical angles between the Ca^{2+}-bound domain of TnC and the two domains of CaM, if they remain after refinement of the two structures, lends credence to the proposed conformational flexibility in this part of these regulatory proteins as suggested previously.[23] Specifically, we have proposed that in the N-terminal domain of TnC, interhelical flexibility may occur with the strong ion pair between Glu64 and Arg84 as a fulcrum as it is formed in both Ca^{2+}-free and the Ca^{2} -bound conformation of this domain.[23,24] The present model of CaM also has this homologous ion pair (Glu54 to Arg74) in the N-terminal domain.

Description of the General Structure of CaM

Ca^{2+}-saturated form

Figure 2a is a stereo-representation of the α-carbon model of the Ca^{2+}-saturated form of CaM. The corresponding α-carbon representation of the $4Ca^{2+}$ form of TnC which formed the starting template for $4Ca^{2+}$ CaM is shown in Figure 2b. The complete tertiary structure of our modeled CaM is represented in Figure 3. The deleted N-terminal 10 residues in CaM is obvious from a comparison of these figures. The overall length of this model of CaM is approximately 62 Å long. The molecule is about 5 Å shorter than TnC owing to the three-residue deletion in the central D/E helical linker (see Fig. 1). This deletion has another effect that is obvious upon detailed comparison of Figure 2a,b; the N-terminal domain is oriented approximately 180° relative to the C-terminal domain in CaM, whereas these domains are approximately 120° to one another in TnC. These structural differences may provide clues to the differences in physiological response exhibited by the two proteins.

The N-terminal domain of CaM consists of four helices, A and B flank Ca^{2+}-binding loop I, C and D flank Ca^{2+}-binding loop II (see Fig. 2a). The D helix runs continuously to join the E helix through the D/E helical linker forming a long 28 residue, central helix linking the two domains. In the C-terminal domain, helices E and F flank binding loop III with the last Ca^{2+}-binding "hand" comprising helix G, loop IV, and helix H. With the interhelical angles of ~ 110° as discussed above, the Ca^{2+}-bound form of CaM is the open conformation of each domain. It is the Ca^{2+}-saturated form of CaM that exhibits the regulatory control on the several enzyme systems studied.

Ca^{2+}-free form

Figure 4 is an α-carbon representation of calcium-free calmodulin. As with the $4Ca^{2+}$ form of CaM, the calcium-free model showed surprisingly few bad contacts or stereochemical conflicts even before energy minimization. The overall root mean square deviation between the initial calcium free model and that after energy minimization was 0.46 Å, and the total energy drop was from 1.50×10^6 to -7.7×10^3 kJ/mol.

The most obvious structural changes which occur in the $4Ca^{2+}$ to $0Ca^{2+}$ transition in the N terminal domain are as follows: Interhelical angles of the A/B, C/D helical pairs increase from 107,110° to 133,151° respectively, similar, of course, to the TnC Ca^{2+}-free N-terminal domain on which it is based. The general effect of increasing the interhelical angles is to result in a more "closed" conformation of the domain,[23] with residues at the N-terminal portion of helix D becoming significantly more buried. Analogous conformational changes in the C-terminal domain cause the burial of residues at the C-terminal portion of the E helix. The overall length of the calcium-free model

a

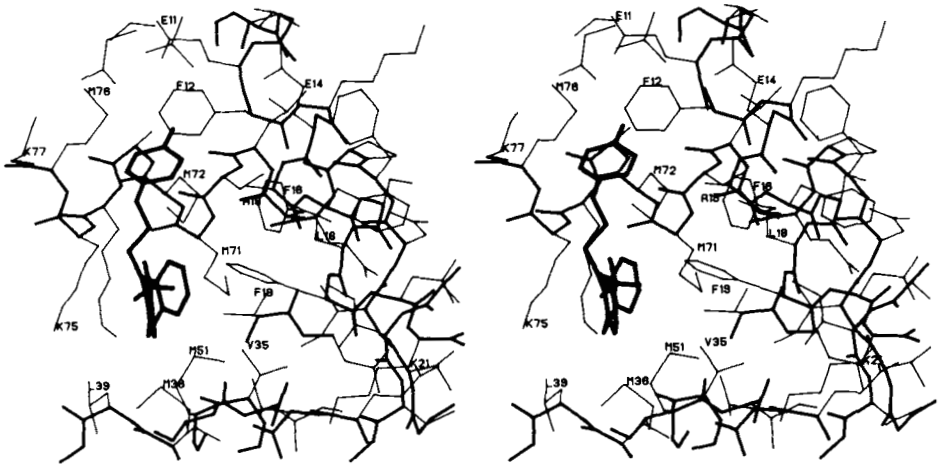

b

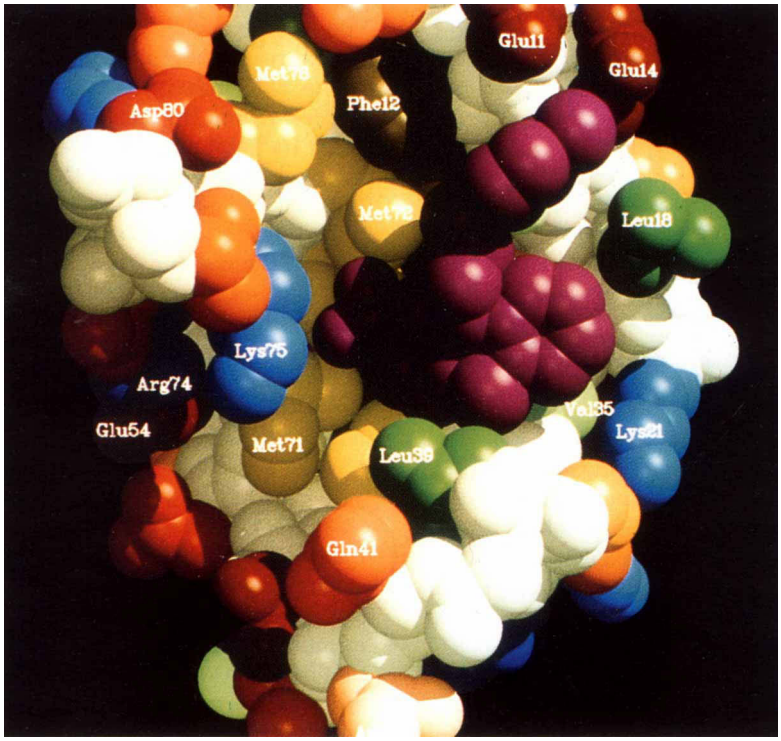

Fig. 9. **a**: A stereographic stick model of the binding of TFP to the N-terminal domain of the $4Ca^{2+}$ CaM model. Main chain and the TFP molecule are in thick lines; side chains are in thin lines. **b**: A space-filling picture of TFP bound in the N-terminal domain of $4Ca^{2+}$ CaM. Amino acid side chains are in standard colors. Negatively charged groups in reds; positively charged groups, blues; methionines, yellow; hydrophobes, green; aromatics, brown. The view is approximately 90° to that in Figure 9a.

of CaM is approximately 58 Å, 4 Å shorter than the $4Ca^{2+}$ model. These values agree well with the results from solution X-ray scattering studies on CaM (J. Trewhella, personal communication).

Analysis of the $4Ca^{2+}$ and $0Ca^{2+}$ molecular models by the algorithm of Kabsch and Sanders[36] indicates that there is very little change in secondary structure between the two forms. The most significant difference is a decrease in α-helicity in the calcium-free form of less than 9%. Our model would suggest, then, that the activation of CaM by the binding of Ca^{2+} is not caused by a large change in α-helicity as much of the earlier CD, UV, and fluorescence work concluded,[37-39] but rather by a reorientation of α-helical

a

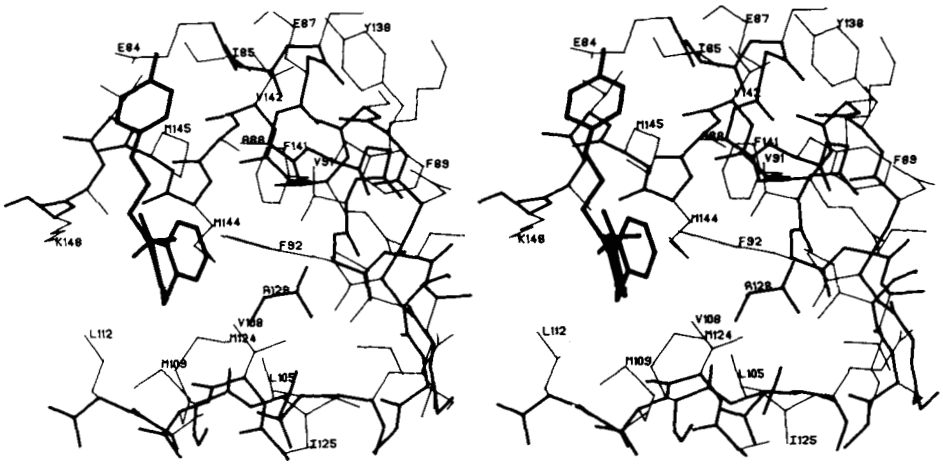

b

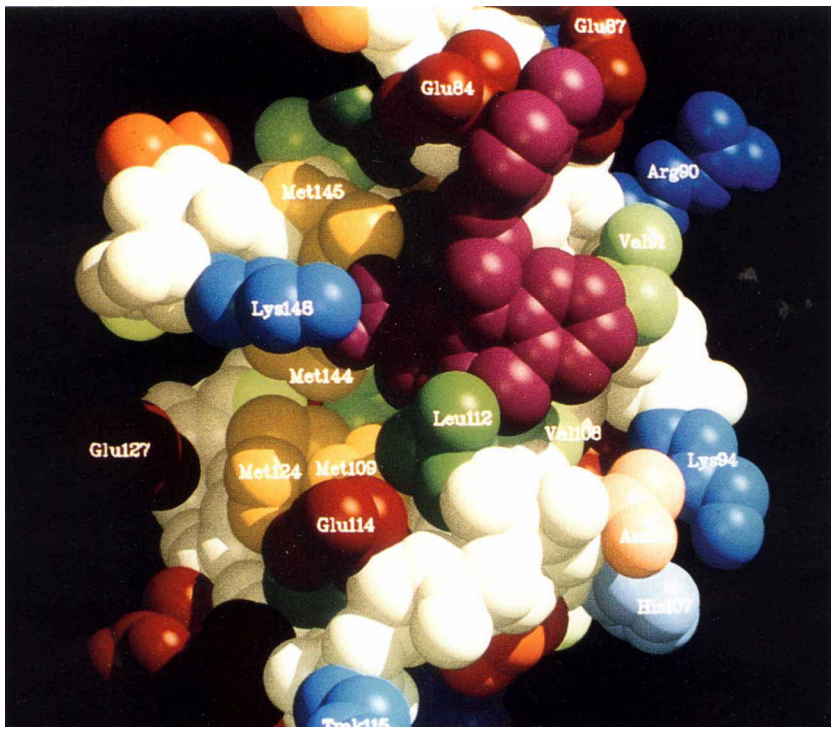

Fig. 10. **a**: A stereographic stick model of the binding of TFP to the C-terminal domain of the $4Ca^{2+}$ CaM model. Main chain and the TFP molecule are in thick lines: side chains are in thin lines. **b**: A space-filling picture of TFP bound in the C-terminal domain. Amino acid colors are as for Figure 9b. The view is approximately 90° to that in Figure 10a.

dipole moments already existing in the Ca^{2+}-free form. Interestingly, results from a recent vacuum-UV circular dichroism study found that the secondary structure of CaM dependend only on ionic strength and was independent of the nature of the cation being used in the system. This implied to the authors that the activation of calmodulin by calcium was due to a structural reorientation rather than to a major change in secondary structure.[40]

Description of the Ca^{2+} Binding Loops

Functionally, the most important regions of CaM are the four Ca^{2+}-binding loops (I–IV) of 12 residues each that the helical pairs A/B, C/D, E/F, and G/H support. An earlier study has shown a very high level of structural conservation in the ligand binding loops of Ca^{2+}-binding proteins.[21] We believe this work, coupled with the relatively high sequence homology

within the binding loops of TnC and CaM, implies a high level of structural validity in this area of our CaM model. A view of binding sites I and II is given in Figure 5a and binding sites III and IV in Figure 5b.

In our model, six coordinating residues in each binding loop (marked by an asterisk in Fig. 1) are suitably oriented to provide oxygen atoms for binding Ca^{2+} ions. Except for the amino acid at position −x, the average Ca^{2+} to oxygen ligand distance is 2.5 Å. In this fifth coordinating position of each loop (Thr28, Asp64, Ser101, Asn137) larger distances of 4.5–4.9 Å from the side chain oxygen atom to the Ca^{2+} ion suggest that the interaction should be mediated via a bridging H_2O molecule as is observed in loops III and IV of TnC. This suggestion for CaM has been made previously, based on a comparison of loop conformations in Ca^{2+}-binding proteins.[21]

Each of the pairs of calcium binding loops are connected and stabilized by hydrogen bonding in a short antiparallel β-sheet conformation. In the N-terminal domain, Ile27 of loop I and Ile63 of loop II share two hydrogen bonds (2.7 Å, 2.8 Å); and similarly in the C-terminal domain, Ile100 of loop III and Val136 of loop IV share two hydrogen bonds (2.8 Å each). This result had been deduced from earlier two-dimensional (2-D) and nuclear Overhauser enhancement (NOE) NMR studies.[41] Additional loop stabilization arises from a series of Asx (side chain oxygen of residue n to main chain nitrogen of residue n+2) and reverse turns as detailed for loops III and IV in TnC.[21,24]

Factors Influencing the Ca^{2+}-Binding Affinity

From the work done to date, it appears that the binding of Ca^{2+} to CaM takes place in two stages.[2–4,41–43] It binds first to sites III and IV in the C-terminal domain; the second stage involves binding Ca^{2+} to sites I and II in the N-terminal domain. It is not yet clear exactly what determines the relative Ca^{2+} affinity of the individual binding loops or whether the loops act in a cooperative manner.

Undoubtedly, there are many factors that determine the binding affinity of Ca^{2+}, not just the nature of the ligands that coordinate directly to the Ca^{2+} ion. It is likely that long-range interactions, electrostatic, van der Waals, and other weak noncovalent interactions will also have an effect on the ease and strength of binding Ca^{2+}. The two different conformations of CaM, the Ca^{2+}-free (closed) and the Ca^{2+}-saturated (open) forms allow us to examine the relative contributions of some of these long-range interactions on Ca^{2+}-binding affinity and allow a comparison of the N-terminal and C-terminal domains of CaM in this regard. Since the measured Ca^{2+} affinities of the two domains are quite similar in CaM, we should expect the weak noncovalent interactions in the two domains also to be similar.

Table I presents the solvent-accessible surface areas, the number of main-chain hydrogen bonds and the number of potential ion pairs for each of the two domains in both of the Ca^{2+}-filled (open) and Ca^{2+}-free (closed) conformations. In going from the open to the closed conformation the total accessible surface area of the N-terminal domain decreases by 10%. The favorable burial of hydrophobic residues accounts for 270 $Å^2$ of the decrease. In the C-terminal domain, there is a corresponding decrease of 11% in the total accessible surface area in going from the open to the closed conformation; 260 $Å^2$ is due to the favorable burial of hydrophobic residues. Thus, it would appear that the closed conformation of the domains is to be preferred. The number of main-chain NH····O hydrogen bonds in both domains does not change significantly in going from the Ca^{2+}-bound (open) to the Ca^{2+}-free (closed) conformation. Thus, our model predicts little change in secondary structure in these two states of the protein, as suggested previously.

Ion pair interactions may be important for protein stability and it is in the number of potential ion pair interactions in CaM that we see differences between the N-terminal domain and the C-terminal domain. There are also differences between the open and closed conformations of the two domains (Table I). In the N-terminal domain of the $4Ca^{2+}$ CaM model, the potential ion pairs include Glu54 (on helix C) and Arg74 (on helix D). This ion pair is homologous to Glu64····Arg84 in TnC and may act as the fulcrum for interhelix flexibility.[23] Another conserved ion pair is Arg37 to Glu45 (see Table I; Figs. 1, 6a). In going to the Ca^{2+}-free (closed) form, there are three additional potential ion pair interactions possible owing to the conformational change of helices B and C (Fig. 6b). One of the new ones is from Glu47 to Lys75. In the closed Ca^{2+}-free conformation the change brings Glu47 into close proximity to Lys75, whereas in the open Ca^{2+}-filled form these residues are 9 Å apart. Of the Ca^{2+}-sensitive regulatory proteins only CaM has a lysine at position 75 (Fig. 1).

In the C-terminal domain in the open Ca^{2+}-filled conformation there is only one potential ion pair (Table I; Figs. 1, 7a). Two additional ion-pair interactions are possible in the closed Ca^{2+}-free conformation (Fig. 7b). Analogous to the Glu47-Lys75 ion pair of the N-terminal domain, Glu120 on helix G moves to interact potentially with Lys148 on helix H (Fig. 7b). Only CaM has this basic residue at position 148.

Overall, the noncovalent interactions in the N-terminal and C-terminal domains are quite similar. The extra potential ion-pair interactions in the N-terminal domain that may stabilize the Ca^{2+}-free (closed) conformation may be correlated with the observation that Ca^{2+} is firstly and preferentially bound to the C-terminal domain in CaM. Site-directed mutagenesis of the CaM gene at these residues providing the ion-pair interactions may provide an indication to the importance of the salt bridges in modifying Ca^{2+} affinity.

Description of the Hydrophobic Patches

The binding and release of calcium to the calcium-binding domains of CaM is known to be the regulating effector of the activity of the various intracellular enzymes with which CaM interacts.[5–16] The results of some studies suggest that many of these enzymes may be binding to a hydrophobic region found in each of the amino- and carboxyterminal domains.[52,69,71,72] Indeed in each of the domains of our Ca^{2+}-saturated CaM model there is a very pronounced hydrophobic patch. The hydrophobic clefts of the N-domain and C-domain face towards each other on opposite sides of the central helix (see Figs. 2a, 3). In each case a number of hydrophobic residues are clustered around a central core composed of the highly conserved loop-stabilizing β-sheet hydrogen bonding pairs Ile27/Ile63 (N-terminal domain) and Ile100/Val136 (C-terminal domain). Table II gives a list of hydrophobic residues in the N-terminal and C-terminal domains along with their relative solvent accessibility values as calculated by the algorithm of Kabsch and Sanders.[36] A view of the N-terminal and C-terminal hydrophobic regions are given in Figures 6a and 7a, respectively. Along the entrance to both apolar cavities are a number of charged acidic residues. In the N-terminal domain these include Glu11, Glu14, Glu47, Asp50, Glu54, and Asp78; and in the C domain these acidic residues include Glu84, Glu87, Glu114, Glu119, Glu120, Glu123, Glu 127. Both the N- and C-terminal hydrophobic patches have a lysine positioned across the opening of the pocket. Lys75 lies across the bottom of the N-terminal pocket and Lys148 extends across and about halfway up the entrance to the C-terminal hydrophobic pocket (Figs. 6a, 7a).

Model of Trifluoperazine Binding to CaM

Since none of the three-dimensional structures of the enzymes that CaM activates are yet known, it seemed premature to model an exact binding site for these enzymes on the hydrophobic patches of CaM. However, it did seem plausible to fit the small, lipophilic drugs which are thought to bind in the apolar pockets and subsequently to inhibit CaM-mediated activation of the various intracellular enzymes mentioned previously. These drugs include the family of antipsychotics called the phenothiazines, most studied of which is trifluoperazine (TFP). Earlier solution work has shown that a CaM molecule has 2 Ca^{2+}-dependent high-affinity ($K_d \sim 5\ \mu M$) sites for TFP.[44] It was suggested that one of the two high-affinity binding sites was located on the N-terminal portion of the molecule and the other on the C-terminal domain of CaM. The affinity of the C-terminal site is at least one order of magnitude greater than that of the N terminal site.[41] It is well documented that the affinity of various phenothiazines for CaM is related to their hydrophobicity.[45–49] Furthermore, studies have shown that a positive charge a certain distance from the phenothiazine ring is crucial for binding to CaM, implying that electrostatic as well as hydrophobic interactions are involved.[46] Ostensibly then, in the binding of TFP to CaM, one would expect the hydrophobic phenothiazine rings (see Fig. 8a) to stack against the residues of the hydrophobic patch, with the positively charged nitrogen of the piperazine moiety extending out of the patch to interact with the negatively charged residues framing the outer rim of the hydrophobic pocket. Additionally, several acetylation studies have shown that Lys75 and Lys148 may be involved at or proximal to the TFP binding site.[50] Recent work using 10-(3-propionyloxysuccinimide)-2-(trifluoromethyl)phenothiazine (POS-TP, see Fig. 8b) showed that Lys148 was labeled at low molar ratios of reagent and Lys75, and Lys77 at higher molar ratios of reagent.[51] This work concluded that binding of POS-TP in the C-terminal domain involved a hydrophobic patch including residues Phe89, Phe92, Phe141, Tyr138, Ile85, Ile25, Val136, Val142 and Met109, Met124, Met144, and Met145. Only a few of these residues agree with our proposed binding site in the C-terminal domain (see below and Table II).

Considering the above observations and by calculating a van der Waals surface portrait of both TFP and CaM ($4Ca^{2+}$), we propose the following TFP binding sites on CaM. In the N-terminal domain the phenothiazine rings of TFP fit nicely into a groove formed by the side chains of Val35, Leu39, Met36, Leu18, Met71, Met72, Phe19, and Ala15 (see Figs. 9a, 10a). The positively charged nitrogen of the piperazine ring can then easily interact with one or both of the acidic side chains of Glu14 and Glu11 which extend off helix A directly outside the hydrophobic patch. Lys75 runs along side the trifluoro group at position 2 of the phenothiazine ring.

In the C-terminal domain hydrophobic patch, the binding site of the phenothiazine ring includes residues Val91, Val108, Leu112, Met109, Phe92, Met144, Met145, and Ala88. In our model Tyr138, Phe89, Phe141, Ile85, Ile125, Val142 and Met124 are too far from the surface of the hydrophobic pocket to interact with TFP. The positively charged nitrogen of the piperazine ring could easily interact with Glu84 and/or Glu87 which extend off the E helix. Lys148 again like Lys75, runs along the side of the trifluoro moiety. Figures 9b and 10b show a view of TFP bound in the C-terminal domain. Figure 11 shows the relative orientation of the two TFP molecules on the whole CaM. Near both TFP-binding sites there is a small cavity formed near the interface of Met71 and Met72 in the N-terminus and Met144 and Met145 in the C-terminus. These cavities could accomodate a propyl or similar-length group on position 3 of the phenothiazine ring. It would be of interest to see if such an analog would invoke tighter binding. From Figures 9a and 10a, one can easily see how an acetylating reagent like POS-TP which has a neutrally charged acetylating succinimide group at the same position as the positively charged piperazine ring in TFP (see Figs.

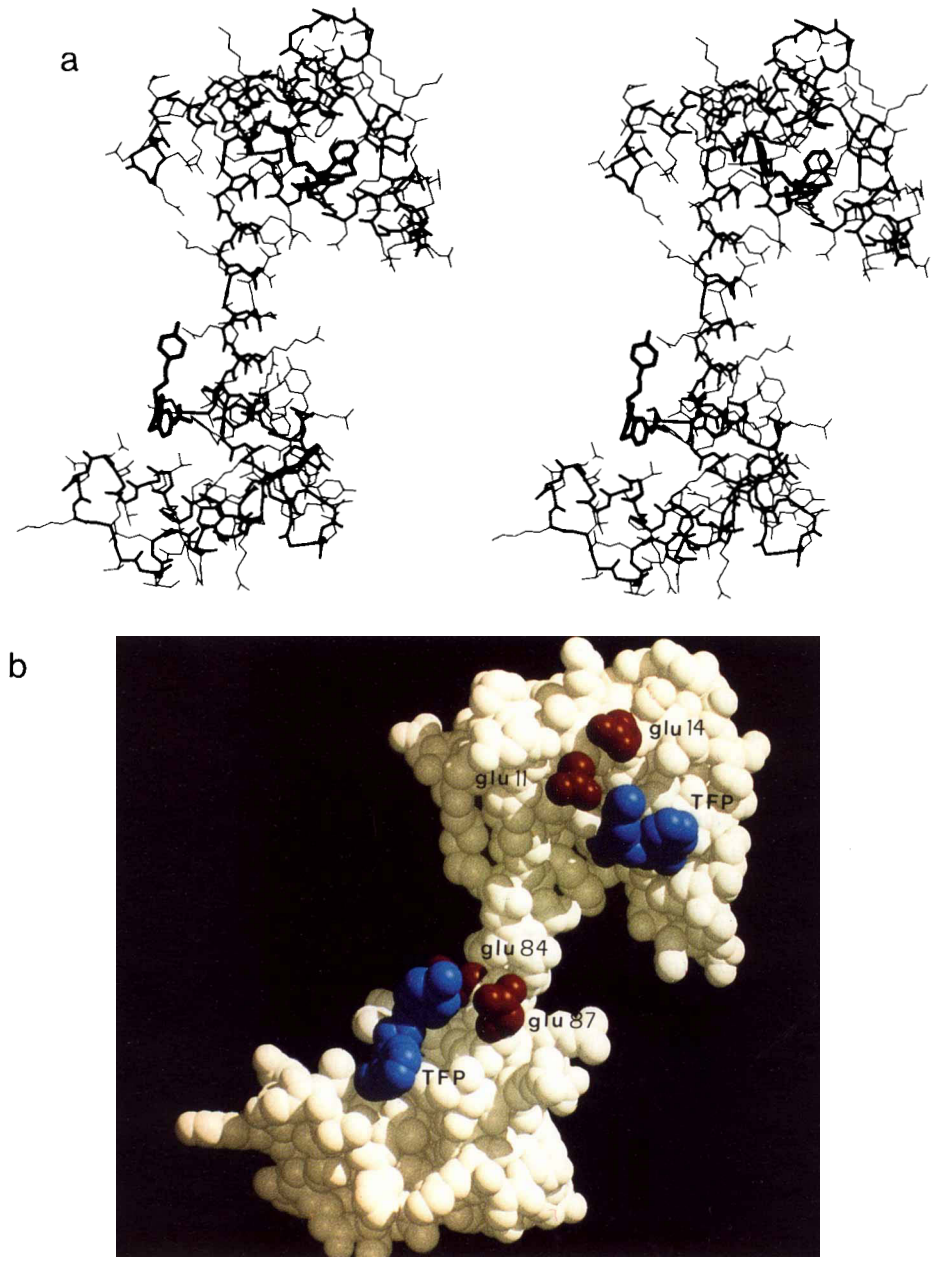

Fig. 11. **a:** A stereo view of the entire calcium-saturated model showing the two proposed binding sites for the antipsychotic drug trifluoperazine. Main chain and TFP molecules are in thick lines; side chains are in thin lines. **b:** A view of calmodulin sharing the two trifluoperazine binding sites. The calmodulin atoms are represented as white spheres with the glutamic acid residues involved in binding the piperazine moiety of TFP in red. The TFP molecules are shown as blue spheres. This figure as well as Figures 9b and 10b were made using "raster 3 D" written by David Bacon.

8a,b) could flip over to acetylate the adjacent lysine (Lys75 or Lys148). It is also clear from these figures that Lys148 is much less sterically hindered than Lys75 and therefore should be more chemically reactive with POS-TP as was observed. Accessibility values[36] for Lys75 and Lys148 in the $4Ca^{2+}$ CaM model are 117 and 225, respectively.

Several studies have indicated that the greater affinity that phenothiazine has for CaM in the presence of Ca^{2+} is the result of modified exposure of hydrophobic patches in the Ca^{2+}-bound conformation.[44,51-55] Comparison of the Ca^{2+}-bound and the Ca^{2+}-free conformation of the N-terminal domain of CaM seems to bear these observations out (see Figs. 6a,b). The hydrophobic patch is significantly more buried in the absence of Ca^{2+}. Of the eight hydrophobic residues involved in binding TFP in the N-terminus of the Ca^{2+}-free state only three residues—Phe19, Leu18, and Ala15—are still suitably exposed to interact with the hydrophobic phenothiazine rings of TFP. Glu11 and Glu14 also retain their relative position to bind the charged piperazine moiety of TFP. Collectively these residues may explain the weak affinity binding of TFP to CaM in the absence of Ca^{2+}. Anal-

ogously in the C-terminal domain, only Phe92, Val91, and Ala88 are sufficiently exposed to bind TFP along with Glu84 and Glu87 (see Figs. 7a,b). Table I shows the change in inaccessibility of key residues of these hydrophobic patches from the calcium-filled to calcium-free state of the N-terminal and C-terminal domains. Residues marked with an asterisk are thought to be involved in TFP binding.

A recent paper using amine-directed chemical modification reagents showed the very high, Ca^{2+}-dependent reactivity of Lys75.[56] It was noted that the adjacent Lys77 had very low reactivity and suggested that this may be due to the fact that Lys77 may be involved in an ion pair with Asp78. The very dramatic calcium dependence of Lys75 reactivity may be explained by our model in two ways. Firstly, as mentioned earlier, in the calcium-filled to calcium-free transition, Glu47 swings in very closely to Lys75 where they could form a salt bridge, thus tying up Lys75 and decreasing its reactivity with reagent. Secondly, and perhaps relatedly, the accessibility value of Lys75 drops dramatically (117→12) in going from Ca^{2+}-bound to the Ca^{2+}-free conformation.

Lys75 and Lys148 have been shown to have increased protection from acetylation when CaM is complexed with myosin light chain kinase (MLCK)[57] and calcineurin.[58] These results coupled with the observed inhibitory effect of TFP on the activation of these enzymes suggests a common binding domain for at least some of the CaM target enzymes. Site-specific mutation of Glu82, Glu83, and Glu84 to lysine residues resulted in the expression of a CaM mutant with a 70% decrease in activation of myosin light chain kinase.[59] Thus, Glu84 may be involved in MLCK binding to CaM as it is for our hypothetical TFP-binding site.

Binding of certain basic amphiphilic α-helical peptides to the C-terminus of CaM can block its ability to activate some target enzymes, including MLCK and phosphodiesterase.[60,61] Tight binding of these amphiphilic helices requires multiple positively charged residues on the peptide, so regions with a high density of negatively charged, acidic residues should attract such peptides. As mentioned earlier, such a region exists as a cluster of glutamic acids surrounding the C-terminal hydrophobic patch. Both α-helical inhibitory peptides, melittin and mastoparan, have lysine and arginine clusters at the termini of their helices and a series of hydrophobic residues predominantly along one face of the helix. Perhaps the binding of these peptides involves the interaction of their basic residues with the acidic patch on CaM and the hydrophobic moieties of the helix pointing in towards the hydrophobic patch of CaM. Such a mode of binding would resemble what we have proposed for TFP and would sterically block the binding of target enzymes to the hydrophobic patch. The Ca^{2+} dependence of binding of both melittin and mastoparan would be due, as with TFP, to their exclusion from the hydrophobic patch as it becomes buried upon Ca^{2+} release.

Other structural features of interest include the following: the clustering of charged acidic residues along the interdomain helix (Asp78, Asp80, Glu82, Glu83, and Glu84, Glu87) and the position of tyrosine residues. Tyr99 is directed from loop III towards the surface, where it is accessible to solvent and is stacked against the side chain of Gln135 (Fig. 5b). Tyr138 points away from loop IV towards helix E, where it comes into close proximity with Phe89 and Phe141. This is consistent with previous solution work that indicated the high pK of Tyr138 was due to its hydrophobic environment.[62] The unique trimethyl-lysine at position 115 is located between helices F and G and does not appear to be interacting with other residues. The single His107 residue on helix F is fully accessible to solvent.

CONCLUSIONS

With the ever-increasing numbers of protein sequences being determined by DNA sequencing methods, there is an increasing need to predict the proteins' three-dimensional structure so that further experiments may be designed. Unfortunately, to date, the secondary-structure prediction algorithms are unreliable.[63] Until fundamental advances in the solution of the protein folding problem are forthcoming the method of comparative molecular modeling[34] provides the greatest promise of success.[35] Furthermore even with the assumption that the secondary structure is correctly predicted, the resulting profile of helices and β-strands is of limited use. Sites of functional importance (active sites on enzymes, effector sites, drug binding sites, etc.) are usually composed of amino acids distant in the primary sequence but brought together by the tertiary folding in the final

As a predictive method, the computer modeling of a protein structure from its sequence and with the knowledge of crystallographically-defined three-dimensional structure of a highly homologous molecule should provide a more accurate and useful description of the molecule. This method is not without its limitations either.[34,35,69] It is the region surrounding those that are highly conserved in the active site that are different among different enzymes. These loops usually provide the substrate specificity and therefore provide the greatest trouble in modeling.[70]

In order to result in as faithful a model as possible, the protein chosen for a template should have as high a sequence homology with the unknown protein as possible. Troponin-C provides such a template for calmodulin. These proteins have 51% sequence identity (70% homology) and many similar physicochemical characteristics. Within the framework of the two caveats we acknowledge, the structure we describe here should be as faithful a description of calmodulin as possible. Our model-building efforts are directly testable. We have deposited the coordinates with the

Brookhaven Protein Data Bank so they can be compared with the coordinates derived from the refined crystal structure of calmodulin when they are available. Lastly, the two proposed binding sites of TFP have given insight into the design of new inhibitors based on the phenothiazine structure that could be more specific and could bind more tightly than existing inhibitory molecules.

REFERENCES

1. Cheung, W.Y. Calmodulin plays a pivotal role in cellular recognition. Science 207:19–27, 1980.
2. Anderson, A., Forsen S., Thulin, E., Vogel, H.J. ^{113}Cd nuclear magnetic resonance studies of proteolytic fragments of calmoludin. Assignment of strong and weak cation binding sites. Biochemistry 22:2309–2313, 1983.
3. Aulabaugh, A., Niemczura, W.P., Gibbons, W.A. High field proton NMR studies of tryptic fragments of calmodulin. A comparison with the native protein. Biochem. Biophys. Res. Commun. 118:225–232, 1984.
4. Klevit, R.E., Dalgarno, D.C., Levine, B.A., Williams, R.J.P. The nature of the Ca^{2+}-dependent conformational change. Eur. J. Biochem. 139:109–114, 1984.
5. Lin, Y.M., Liu, Y.P., Cheung, W.Y. Cyclic 3′,5′-nucleotide phosphodiesterase. Purification, characterization, and active form of the protein activator from bovine brain. J. Biol. Chem. 249:4943–4954, 1974.
6. Teo, T.S., Wang, J.H. Mechanisms of activation of a cyclic adenosine 3′,5′ monophosphate phosphodiesterase from bovine heart by calcium ions. J. Biol. Chem. 248:5950–5955, 1973.
7. Anderson, J.M., Cormier, M.J. Calcium-dependent regulator of NAD kinase in higher plants. Biochem. Biophys. Res. Commun. 84:595–602, 1978.
8. Hathaway, D.R., Adelstein, R.S. Human platelet myosin light chain kinase requires the calcium-binding protein calmodulin for activity. Proc. Natl. Acad. Sci. U.S.A. 76:1653–1657, 1979.
9. Dabrowska, R., Sherry, J.M.F., Avomatorio, D.K., Hartshorne, D.J. Modulator protein as a component of the myosin light chain kinase from chicken gizzard. Biochemistry 17:253–258, 1978.
10. Waisman, D.M., Singh, T.J., Wang, J.N. The modulator-dependent protein kinase. J. Biol. Chem. 253:3387–3390, 1978.
11. Lynch, T.J., Cheung, W.Y. Human erythrocyte Ca^{2+}, Mg^{2+}-ATPase: Mechanism of stimulation by calcium. Arch. Biochem. Biophys. 194:165–170, 1979.
12. Hanahan, D.J., Tavern, R.D., Flynn, D.D., Eckholm, J.E. The interaction of Ca^{2+}/Mg^{2+} ATP'ase activator protein and Ca^{2+} with human erythrocyte membranes. Biochem. Biophys. Res. Commun. 84:1009–1015, 1978.
13. Brostrom, M.A., Brostrom, C.O., Breckenridge, B.M., Wolff, D.J. Regulation of adenylate cyclase from glial tumor cells by calcium and a calcium-binding protein. J. Biol. Chem. 251:4744–4750, 1976.
14. Brostrom, M.A., Brostrom, C.O., Wolff, D.J. Calcium-dependent adenylate cyclase from rat cerebral cortex: Activation by guanine nucleotides. Arch. Biochem. Biophys. 191:341–350, 1978.
15. Westcott, K.R., Laporte, D.C., Storm, D.R. Resolution of adenylate cyclase sensitive and insensitive to Ca^{2+} and calcium-dependent regulatory protein (CDR) by CDR-sepharose affinity chromatography. Proc. Natl. Acad. Sci. U.S.A. 76:204–208, 1979.
16. Cohen, P., Burchell, A., Foulkes, J.G., Cohen, P.T.W., Vanaman, T.C., Nairn, A.C. Identification of the Ca^{++}-dependent modulator protein as the fourth subunit of rabbit skeletal phosphorylase kinase. FEBS Lett. 92:287–289, 1978.
17. Crow, T.J., Deakin, J.W.F., Johnstone, E.C. Stereospecificity and clinical potency of neuroleptics. Nature 267:183–184, 1977.
18. Earl, C.Q., Prosialeck, W.C., Wiess, B. Inhibition of calmodulin activity by α-adrenergic antagonists. Fed. Proc. 41:1565–1569, 1982.
19. Kretzinger, R.H. Structure and evolution of calcium-modulated proteins. CRC Crit. Rev. Biochem. 8:119–174, 1980.
20. Herzberg, O., James, M.N.G. Structure of the calcium regulatory muscle protein troponin-C at 2.8 Å resolution. Nature 313:653–659, 1985.
21. Herzberg, O., James, M.N.G. Common structural framework of the two Ca^{2+}/Mg^{2+} binding loops of troponin C and other Ca^{2+} binding proteins. Biochemistry 24:5298–5302, 1985.
22. Herzberg, O., James, M.N.G. Refined crystal structure of troponin C from turkey skeletal muscle at 2.0 Å resolution. J. Mol. Biol. (Submitted).
23. Herzberg, O., Moult, J., James, M.N.G. A model for the Ca^{2+} induced conformational transition of troponin-C and other Ca^{2+} binding proteins. J. Biol. Chem. 261:2638–2644, 1986.
24. Herzberg, O., Moult, J., James, M.N.G. Calcium binding to skeletal muscle troponin-C and the regulation of muscle contraction. Evered, D., Whelan, J. (eds.) In: "Calcium and Cell Function" (Ciba Foundation Symposium 122). Chichester: Wiley. 1986. 120–139.
25. Stevens, F.C., Walsh, M., Ho, H., Teo, J.H., Wang, J.H. Comparison of calcium-binding proteins. Bovine heart and brain protein activators of cyclic nucleotide phosphodiesterase and skeletal muscle troponin C. J. Biol. Chem. 251:4495–4500, 1976.
26. Watterson, D.M., Harrelson, W.G. Jr., Keller, P.M., Sharief, F., Vanaman, T.C. Structural similarities between the Ca^{2+}-regulatory proteins of 3′5′-cyclic nucleotide phosphodiesterase and actomyosin ATP'ase. J. Biol. Chem. 251:4501–4513, 1976.
27. Amphlett, G.W., Vanaman, T.C., Perry, S.V. Effect of the troponin C-like protein from bovine brain (brain modulator protein 1) on the Mg^{++}-stimulated ATPase of skeletal muscle actomyosin. FEBS Lett. 72:163–168, 1976.
28. Castellani, L., Morris, E.P., O'Brien, E.J. Calmodulin as a model for troponin C. Biochem. Biophys. Res. Commun. 96:558–565, 1980.
29. Babu, Y.S., Sack, J.S., Greenhough, T.J., Bugg, C.E., Means, A.R., Cook, W.J. Three dimensional structure of calmodulin. Nature 315:37–40, 1985.
30. O'Neil, K.T., Delgrado, W.F. A predicted structure of calmodulin suggests an electrostatic basis for its function. Proc. Natl. Acad. Sci. U.S.A. 82:4954–4958, 1985.
31. Aulabaugh, A., Niemczura, W.P., Blundell, T.L., Gibbons, W.A. A study of the interactions between residues in the C-terminal half of calmodulin by one and two-dimensional NMR methods and computer modeling. Eur. J. Biochem. 143:409–418, 1984.
32. Van Gunsteren, W.F., Berendsen, H.J.C., Gromos Laboratory of Physical Chemistry, University of Groningen, Nijenborgh 16, 9747 AG Groningen, The Netherlands, 1984.
33. Van Gunsteren, W.F., Karplus, M. Effect of constraints on the dynamics of macromolecules . Macromolecules 15:1528–1544, 1982.
34. Greer, J. Comparative model-building of the mammalian serine proteases. J. Mol. Biol. 153:1027–1042, 1981.
35. Read, R.J., Brayer, G.D., Jurášek, L., James, M.N.G. Critical evaluation of comparative model building of *Streptomyces griseus* trypsin. Biochemistry 23:6570–6575, 1984.
36. Kabsch, W., Sanders, C. Dictionary of protein secondary structure: pattern recognition of hydrogen bonded and geometrical features. Biopolymers 22:2577–2637, 1983.
37. Van Eerd, J.P., Kawasaki, Y. Ca^{++} induced conformational changes in the Ca^{++} binding component of troponin C. Biochem. Biophys. Res. Commun. 47:859–865, 1972.
38. Murray, A.C., Kay, C.M. Hydrodynamic and optical properties of troponin C. Demonstration of a conformational change upon binding calcium ion. Biochemistry 11:2622–2627, 1972.
39. Johnson, J.D., Potter, J.D. Detection of two classes of Ca^{2+} binding sites in troponin C with circular dichroism and tyrosine fluorescence. J. Biol. Chem. 253:3775–3777, 1978.
40. Hennessey, J.D., Parthasavathy, M.W., Johnson, C.W., Malencik, D.A., Anderson, S.A., Schimerlik, M.I., Shalifin, Y. Conformational transitions of calmodulin as studied by vacuum-U.V. CD. Biopolymers 26:561–571, 1987.
41. Dalgarno, D.C., Klevit, R.E., Levine, B., Williams, R.J.P., Dobrowolski, Z. ^{1}H-NMR studies of calmodulin. Resonance assignments by use of tryptic fragments. Eur. J. Biochem. 138:281–289, 1987.

42. Ikura, M., Hiraoki, T., Mikichi, K., Mikun, T., Yazawa, M., Yagi, K. Nuclear magnetic resonance studies on calmodulin: Ca^{2+}-induced conformational change. Biochemistry 22:2573–2579, 1983.
43. Ikura, M., Hiraoki, T., Minowa, O., Yamaguchi, N., Yazawa, W., Yagi, K. Nuclear magnetic resonance studies on calmodulin: Ca^{2+} dependent spectral change of proteolytic fragments. Biochemistry 23:3121–3128, 1984.
44. Dalgarno, P.C., Klevit, R.E., Levine, B.A., Scott, G.M., Williams, R.J.P. The nature of trifluoperazine binding sites on calmodulin and troponin-C. Biochim. Biophys. Acta 791:164–172, 1984.
45. Richman, P.G., Klee, C.B. Conformation-dependent nitration of the protein activator of cyclic adenosine 3′,5′-monophosphate phosphodiesterase. Biochemistry 17:928–935, 1978.
46. Prozialeck, W.C., Weiss, B. Inhibition of calmodulin by phenothiazines and related drugs: structure-activity relationships. J. Pharmacol. Exp. Ther. 222:509–514, 1982.
47. Levin, R.M., Weiss, B. Specificity of the binding of trifluoperazine to the calcium-dependent activator of phosphodiesterase and to a series of calcium-binding proteins. Biochim. Biophys. Acta 540:197–204, 1978.
48. Levin, R.M., Weiss, B. Binding of trifluoperazine to the calcium-dependent activator of cyclic nucleotide phosphodiesterase. Mol. Pharmacol. 13:690–694, 1977.
49. Levin, R.M., Weiss, B. Selective binding of anti-psychotics and other psychoactive agents to the calcium-dependent activator of cycle nucleotide phosphodiesterase. J. Pharmacol. Exp. Ther. 208:454–459, 1979.
50. Giedroc, D.P., Sinha, S.K., Brew, K., Puett, D. Differential trace labelling of calmodulin: Investigation of binding sites and conformational states by individual lysine reactivities. J. Biol. Chem. 260:13406–13413, 1985.
51. Faust, F., Slisz, M., Jarrett, M. Calmodulin is labelled at lysine 148 by a chemically reactive phenothiazine. J. Biol. Chem. 262:1938–1941, 1987.
52. Laporte, D.C., Wierman, B.M., Storm, D.R. Calcium-induced exposure of a hydrophobic surface on calmodulin. Biochemistry 19:3814–3819, 1980.
53. Tanaka, T., Hidaka, H. Hydrophobic regions function in calmodulin-enzyme(s) interactions. J. Biol. Chem. 255: 11078–11080, 1980.
54. Klevit, R.E., Levine, B.A., Williams, R.J.P. A study of calmodulin and its interaction with trifluoperazine by high resolution ^1H NMR spectroscopy. FEBS Lett. 123:25–29, 1981.
55. Krebs, J., Carafoli, E. Influence of Ca^{2+} and trifluoperazine on the structure of calmodulin. Eur. J. Biochem. 124:619–627, 1982.
56. Mann, D., Vanaman, T.C. Chemical modification as a probe of calmodulin function. Methods Enzymol. 139:417-433, 1987.
57. Jackson, A.E., Carraway, K.L., Puett, D., Brew, K. Effects of the binding of myosin light chain kinase on the reactivities of calmodulin lysines. J. Biol. Chem. 261:12226–12232, 1986.
58. Manalan, A.S., Klee, C.B. Affinity selection of chemically modified proteins: Role of lysyl residues in the binding of calmodulin to calcineurin. Biochemistry 26:1382–1390, 1987.
59. Craig, T.A., Watterson, D.M., Prendergrast, F.G., Haiech, J., Roberts, D.M. Site specific mutagenesis of the α-helices of calmodulin. J. Biol. Chem. 262:3278–3287, 1987.
60. Malencik, D.A., Anderson, S.R. Binding of simple peptides, hormones and neurotransmitters by calmodulin. Biochemistry 21:3480–3486, 1982.
61. Malencik, D.A., Anderson, S.R. Peptide binding by calmodulin and its proteolytic fragments and by troponin C. Biochemistry 23:2420–2428, 1984.
62. Seamon, K.B. Calcium and magnesium dependent conformational states of calmodulin as determined by nuclear magnetic resonance. Biochemistry 19:207–215, 1980.
63. Kabsch, W., Sander, C. How good are predictions of protein secondary structure? FEBS Lett. 155:179–182, 1983.
64. Collins, J.N., Potter, J.D., Norn, J.H., Wilshire, G., Jackman, N. The amino acid sequence of rabbit skeletal muscle troponin C: gene replication and homology with calcium-binding proteins from carp and hake muscle. FEBS Lett. 36:268–272, 1973.
65. Wilkinson, J.M. The amino acid sequence of troponin C from chicken skeletal muscle. FEBS Lett. 70:254–256, 1976.
66. Van Eerd, J.P., Takahashi, K. Determination of the complete amino acid sequence of bovine cardiac troponin C. Biochemistry 15:1171–1180, 1975.
67. Watterson, D.M., Sharief, F., Vanaman, T.C. The complete amino acid sequence of the Ca^{2+}-dependent modulator protein (calmodulin) of bovine brain. J. Biol. Chem. 255:962–975, 1980.
68. McDowell, J.J.H. Trifluoperazine hydrochloride, a phenothiazine derivative. Acta Cryst. B36:2178–2181, 1980.
69. Jarret, H. The synthesis and reaction of a specific affinity label for the hydrophobic drug-binding domains of calmodulin. J. Biol. Chem. 259:10136–10144, 1984.
70. Moult, J., James, M.N.G. An algorithm for determining the conformation of polypeptide segments in proteins by systematic search. Proteins: Structure, Function Genet. 1:46–163, 1986.
71. Gietzen, K., Sadorf, I., Bader, H. High affinity binding of the mastoparons by CaM. Biochem. J. 207:541–548, 1982.
72. Malencik, D.A., Anderson, S.R. A model for the regulation of the calmodulin-dependent enzymes erythrocyte Ca^{2+}-transport ATPase and brain phosphodiesterase by activators and inhibitors. Biochem. Biophys. Res. Commun. 114: 50–56, 1983.